Supplementary Information for:

Insights into autophagosome biogenesis from structural and biochemical analyses of the ATG2A-WIPI4 complex

Saikat Chowdhury, Chinatsu Otomo, Alexander Leitner, Kazuto Ohashi, Ruedi Aebersold, Gabriel C. Lander and Takanori Otomo

Corresponding authors: Gabriel C. Lander and Takanori Otomo
Email: glander@scripps.edu; totomo@scripps.edu

This PDF file includes:

Supplementary Materials and Methods
Figs. S1 to S4
Tables S1
Captions for Movie S1
References for SI reference citations

Other supplementary materials for this manuscript include the following:

Movies S1

Supplementary Materials and Methods

Protein expression and purification

The DNA sequence coding human WIPI4 was cloned into pACEBac1 vector (1) with a PreScission protease-cleavable N-terminal histidine tag. Baculoviruses were generated from the resulting vector in *Spodoptera frugiperda* 9 (Sf9) cells using multibac system (1). Sf9 cells infected with the baculoviruses were grown at 27˚C, harvested 48 hours post-infection, resuspended in lysis buffer 20 mM HEPES pH7.5, 150 mM NaCl, 0.5 mM TCEP, and 1 mM PMSF, and lysed using a Dounce homogenizer. The lysate was clarified by centrifugation at 40,000 × *g*, and the protein in the supernatant was purified by nickel affinity chromatography, followed by anion exchange chromatography on a Source 15Q column (GE Healthcare) and size exclusion chromatography on a Superdex 200 column (GE Healthcare) equilibrated with 10 mM HEPES pH7.5, 300 mM NaCl, and 0.5 mM TCEP. The eluted protein was concentrated, flash-frozen in liquid nitrogen, and stored in a -80˚C freezer until use. WIPI4 without the histidine tag was generated by cleaving the tag between the nickel affinity and the anion exchange chromatography steps. ATG18 cDNA sequence was cloned into pFastBacHT (Life Technologies) with a TEV protease-cleavable N-terminal tag. His-ATG18 protein was expressed in Sf9 cells using baculoviruses generated with this vector as described above and purified by nickel affinity, Source 15Q anion exchange, Phenyl HP hydrophobic Sepharose (GE Healthcare) and Superdex 200 size exclusion chromatographic methods, followed by removal of the histidine tag by TEV protease. Upon digestion, TEV protease was removed by second nickel affinity chromatography (TEV is tagged with the histidine tag). The ATG18 protein in the flow-through of the nickel beads was frozen and stored as described above.

Human ATG2A and *Sc*ATG2 cDNA sequences were cloned into pACEBac1 vector with a TEV-cleavable glutathione-S-transferase (GST) and a PreScission-cleavable Twin-StrepII (TS) tags at the N- and C-terminus, respectively. Baculoviruses were generated using the resulting vectors and the proteins were expressed in Sf9 cells as described above. Cells were harvested, resuspended in lysis buffer 20 mM HEPES pH7.5, 150 mM NaCl, 0.5 mM TCEP, and 1 mM PMSF, and lysed by adding 2% Triton X-100, followed by 1 hour stir-mixing at 4˚C. The lysate was clarified by centrifugation at 40,000 × *g*. The supernatant was diluted to reduce the concentration of Triton X-100 below 1% and to contain total 500 mM NaCl and then mixed with Glutathione Sepharose beads (GE Healthcare) in a batch mode. After a 4-hour incubation at 4˚C, the beads were collected by centrifugation and transferred into a gravity column. The beads were washed with buffer containing 20 mM Tris-HCl pH 8.0, 500 mM NaCl, 0.5 mM TCEP, 25% glycerol, and 0.1% Triton X-100, then TEV protease was added to the beads for removal of the GST tag. The cleaved protein was eluted in the same buffer, flash-frozen in liquid nitrogen and stored at -80˚C until further use. For negative stain EM analysis of ATG2A alone, the protein solution was thawed and loaded onto Strep-Tactin Superflow affinity chromatography beads (IBA). The beads were washed extensively with 100 mM Tris-HCl pH 8.0, 150 mM NaCl, 0.5 mM TCEP to remove Triton X-100, followed by elution with the same buffer containing additional 5 mM desthiobiotin. For the negative stain EM analysis of the ATG2A-WIPI4 and *Sc*ATG2-ATG18 complexes, the Strep-Tactin Superflow beads loaded with hATG2A or *Sc*ATG2 were mixed with an excess amount of WIPI4 or ATG18. After a brief incubation, the beads were washed and eluted as described above. The proteins eluted from the Strep-Tactin Superflow were used immediately for preparations of negative stain EM grids. For membrane binding and tethering assays, the elution from Glutathione Sepharose beads was thawed and loaded onto Strep-Tactin XT Superflow beads (IBA). The beads were washed, and protein was eluted similarly as described above except that 50 mM biotin instead of desthiobiotin was used for the elution. PreScission protease was added to the elution for removal of the C-terminal TS tag. The cleaved tag and biotin were removed by dialysis with three-time buffer exchanges. The purified ATG2A protein was used immediately for biochemical assays. The ATG2A^{12xD} mutant, in which all of the aspartic acid mutations in H2 and H3 regions described below

were incorporated (total 12 mutations), was expressed and purified from the baculovirus-infected Sf9 cells in the same manner as the wild-type protein.

For the N-terminal MBP labeling, the DNA sequence coding ATG2A was cloned into pFastBacHT vector with a non-protease-cleavable N-terminal MBP tag and a TEV-cleavable C-terminal histidine tag. The MBP-ATG2A-His protein was expressed in insect cells similarly as described above. 10 mM imidazole pH8.0 was added to the clarified cell lysate, which had been prepared as described above, and the lysate was mixed with TALON cobalt affinity beads (Clontech Laboratories). After a one-hour incubation at 4˚C, the beads were collected and washed with 20 mM Tris-HCl pH 7.5, 300 mM NaCl, 10 mM imidazole, 0.5 mM TCEP, 20% glycerol, and 0.05% Triton X-100, followed by elution with the same buffer except containing 150 mM imidazole. The eluate was then loaded onto Amylose affinity beads (New England Biolabs). After a wash with 20 mM Tris-HCl pH 8.0, 500 mM NaCl, 0.5 mM TCEP, 20% glycerol, and 0.1% Triton X-100, an excess amount of WIPI4 was added to the beads, followed by a brief incubation and rewashed with the 20 mM Tris-HCl pH 7.5, 150 mM NaCl, 0.5 mM TCEP, 10% glycerol, and 0.05% Triton X-100. The protein was eluted with the same buffer containing additional 10 mM maltose and used immediately for EM grid preparation.

For the internal MBP labeling, the DNA fragment coding the amino acid sequence Gly-Gly-Ser-Gly-Ala-Ser-MBP sequence-Ser-Gly-Gly-Ser-Gly-Gly was inserted into the positions between 1224 and 1225 (in ATG2_CAD), 1344 and 1345, 1373 and 1374, 1503 and 1504, and 1829 and 1830 (between the CLR and ATG_C) of ATG2A in pACEBac1 vector harboring GST-ATG2A-TS described above. The MBP-inserted proteins were purified similarly as the wild-type by Glutathione Sepharose chromatography, followed by on-beads TEV cleavage for removal of the N-terminal GST tag. Before the TEV addition, the beads were washed with 20 mM Tris-HCl pH 7.5, 1 M NaCl, 20% glycerol, 0.5 mM TCEP, and 0.026% DDM. The cleaved proteins were eluted in this buffer and concentrated, and then injected into Superose 6 size exclusion column equilibrated with the same buffer. The fractions containing MBP-inserted ATG2A were pooled and concentrated. An excess amount of WIPI4 was added and the complex was isolated in Superose 6 size exclusion column equilibrated with 20 mM Tris-HCl pH 7.5, 500 mM NaCl, 0.5 mM TCEP, 10% glycerol, and 0.026% DDM. The proteins eluted from this column were immediately used for the preparation of EM grids.

For the C-terminal MBP labeling, the DNA sequence coding MBP was inserted between PreScission protease recognition sequence and TS tag of the pACEBac1 vector harboring GST-ATG2A-TS fusion. The GST-ATG2A-MBP-TS protein was expressed and purified in the same manner as the wild-type ATG2A. Before the elution from Strep-Tactin XT affinity beads, WIPI4 was added to form the complex. After wash with 20 mM Tris-HCl pH 7.5, 150 mM NaCl, 0.5 mM TCEP, 10% glycerol, and 0.026% DDM, the protein was eluted in the same buffer supplemented with 50 mM biotin and used for EM analysis.

The DNA sequences coding the CLR fragments (CLR: residues 1723-1819; H1: 1721-1739; H2: 1751-1774; H3: 1777-1819) were cloned into pET Duet-1 vector (Novagen) with a TEV-cleavable N-terminal His-MBP tag and the *Mycobacterium xenopi* gyrA intein-chitin binding domain (CBD) fusion unit from TXB1 vector (New England Biolabs). *E. coli* BL21(λDE3) cells were transformed with the resulting vector harboring His-MBP-CLR-intein-CBD under T7 promoter and grown in Terrific broth medium at 37˚C. Protein expression was induced by adding 0.4 mM IPTG when OD_{600} reached ~2.4. Cells were further grown for overnight at 22C˚, harvested, resuspended in 20 mM Tris-HCl pH 8.5, and 500 mM NaCl, and lysed using an Avestin C3 homogenizer. The lysate was clarified by centrifugation at 40,000 × *g*. 0.2 (v/v) % Triton X-100 was added the supernatant, which was mixed with chitin affinity beads (New England Biolabs) in a batch mode for 2 hours at 4˚C. The beads were collected into a gravity column and washed with 20 mM Tris-HCl pH 8.5, 500 mM NaCl, and 0.1% Triton X-100. 40-50 mM DTT was added to the washed beads for intein cleavage and the beads were incubated at room temperature for initial 5 hours, followed by overnight incubation at 4˚C. Subsequently, His-MBP-CLR was eluted

in the same buffer, concentrated and injected into a Superdex 200 size exclusion column equilibrated with 20 mM Tris-HCl pH 7.5, 500 mM NaCl, and 0.05% Triton X-100. The fractions containing the proteins were loaded onto Amylose affinity beads (New England Biolabs) and washed with 20 mM Tris-HCl, 150 mM NaCl extensively to remove detergents. The proteins were eluted in the same buffer supplemented with 10 mM maltose and used immediately for membrane binding assays and CD experiments. The MBP-fused H2 and H3 fragments with 4 (V1754D/F1761D/L1765D/Y1772D) and 8 (L1778D/L1782D/F1789D/L1800D/L1804D/I1808D/V1815D/L1819D) aspartic acid mutations were generated in the same manner as the wild-type fragments as described above.

The DNA sequence coding the residues 1358-1404 of ATG2A (the WIPI4-binding fragment) was cloned into pET vector with a His-GB1 N-terminal tag. The fusion protein was expressed in *E. coli* BL21(λDE3) similarly as described above for the CLR fragments and purified by nickel affinity chromatography, followed by size exclusion chromatography on a Superdex 200 column. The purified proteins were concentrated and stored at -80˚C until use.

Affinity capture binding assay of the ATG2-WIPI4 and ATG2-ATG18 complexes

Strep-Tactin Superflow beads loaded with ATG2A were mixed with an excess amount of His-WIPI4 in buffer containing 20 mM HEPES pH 7.5, 150 mM NaCl, 0.5 mM TCEP, 20% glycerol, and 0.1% Triton X-100. Beads were collected by centrifugation and washed with the same buffer three times. Proteins were eluted with the same buffer containing additional 5 mM desthiobiotin. The contents of the elution were examined by SDS-PAGE analysis (Fig. 1B). The control was carried out using the beads without ATG2A.

Reconstitution of the ATG2A-WIPI4-SUV complex for negative stain EM analysis

The lipid mixture (75% DOPC/25% DOPS) was dried under nitrogen gas and vacuum dried. The obtained lipid film was dissolved in a buffer 20 mM Tris pH 8.0, 150 mM NaCl, and 50 mM sodium cholate and dialyzed against the same buffer without sodium cholate. This dialysis procedure produced SUVs that were more homogenous than sonication method. The diameter of the SUVs was ~30 nm as determined by EM and DLS. To reconstitute the protein-SUV complex, ATG2A-TS was loaded onto StrepTactin beads. After a wash with 20 mM Tris pH 8.0, 150 mM NaCl, and 0.5 mM TCEP, WIPI4 was added to the beads. After 5 min incubation, the beads were rewashed, and the liposomes were added, followed by another 10 min incubation. The beads were then washed with five column volumes, and the protein was eluted with 5 mM desthiobiotin. The eluted ATG2A-WIPI4-SUV complex was observed by negative stain EM as described below. Mixing the purified ATG2A-WIPI4 complex and the SUVs in solution also yielded a similar sample as determined by the negative stain EM while the data was collected using the sample reconstituted on beads (see below).

Negative Stain Electron Microscopy

Sample preparation

Continuous carbon grids for negative stain analyses were prepared by evaporating carbon onto nitrocellulose-coated 400 mesh Cu-Rh maxtaform grids (Electron Microscopy Sciences). For preparing each stained grid, a freshly glow-discharged grid was placed inversely on a 4 µL droplet of purified protein sample, which was sitting on a sheet of Parafilm, and incubated for 2 minutes. Most of the sample was wicked off with a filter paper (Whatman No. 1), and grids were immediately placed onto the surface of a 4 µL droplet of 2% (w/v) uranyl formate solution. After 5 seconds incubation, the grid was removed from the droplet, and excess stain was wicked off from the grid using filter paper. This staining step was repeated two more times. In the last staining step, the stain incubation time was extended to 30 seconds to thoroughly embed the protein sample in stain. Finally, after wicking off bulk stain, the

grid was completely air-dried on a piece of Parafilm. Grids for the protein-liposome complex were prepared similarly except that the initial incubation with the protein-liposome sample was extended to 5 minutes and 1% (w/v) uranyl acetate solution was used for staining.

Data acquisition

All the electron microscopy data were collected on a Tecnai Spirit (FEI) transmission electron microscope operating at 120keV, using a Tietz F416 CMOS, 4K × 4K camera (TVIPS). Data were acquired using the Leginon automated data acquisition system(2), using a nominal magnification of 52,000 ×, which yielded a pixel size of 2.05 Å at the detector level. Micrographs were collected using a total dose of ~30 electrons/$Å^2$, and with a defocus ranging from 1 µm to 1.5 µm. 1,407, 590, 441, 414, 626, 348, 440, 291, 409 and 1,805 micrographs were collected for ATG2A-WIPI4 complex, ATG2A alone, N-terminal-MBP tagged ATG2A-WIPI4 complex, C-terminal MBP-tagged ATG2A-WIPI4 complex, MBP tag at CADS (position 1224) of ATG2A-WIPI4 complex, MBP tag at position 1829 of ATG2A-WIPI4 complex, MBP tag at position 1503 of ATG2A-WIPI4 complex, MBP tag at position 1344 of ATG2A-WIPI4 complex, MBP tag at position 1373 of ATG2A-WIPI4 complex, and ATG2A-WIPI4 complex associated with liposome datasets respectively.

Image Processing

The Appion image-processing pipeline (3) was used to process the micrographs for all the datasets. CTFFind3 (4) was used for determining the contrast transfer function (CTF) of each micrograph. Particles were picked from the micrographs using Difference of Gaussians (DoG)-based automated particle picker (5), except the liposome-associated ATG2A-WIPI4 dataset, for which particles were manually picked from micrographs using the Manual Picker program in Appion. The phases of the micrographs were flipped using EMAN (6), and particles were extracted using a box size of 192 × 192 pixels for ATG2A, the ATG2A-WIPI4 complex, and yeast ATG2-ATG18 complex. A box size of 224 × 224 pixels was used for the extraction of all MBP-tagged ATG2A-WIPI4 complexes. For the liposome-bound ATG2A-WIPI4 complex dataset, a 160 × 160 pixel box, which incorporated the entire protein but only a fraction of liposome densities, was used. Particles for all the datasets were binned by a factor of two to speed up image processing. The extracted particle datasets were subjected to a topology-based reference-free 2D classification (7) in Appion, which was used to remove non-particle features and aggregates. The resulting stacks were used for subsequent analyses. To aid visualization of the flexible attachment of WIPI4 to ATG2A, we performed a masked classification that focused on the region surrounding the WIPI4 density using the Maskiton (8) web-based classification server on a pre-aligned stack of particles. The resulting 2D classes were used to create the movie depicting the flexible attachment of WIPI4 to ATG2 (Movie S1).

RELION1.4 (9) was used for 3D analyses of ATG2A and ATG2A-WIPI4 datasets, which contained 37,021 and 75,239 particles respectively. Particle stacks were normalized by eliminating pixels with values above or below 4.5σ of the mean pixel value using the normalization function in RELION, prior to 3D analysis. For 3D reconstruction of the ATG2A-WIPI4 dataset, a cylinder with similar dimensions (220Å in length and 50Å in diameter) as ATG2A was created using the "MO 3" function in the SPIDER (10) image processing program, which was used as an initial volume for a single-class initial 3D classification run in RELION. The resulting 3D class was used as an initial model for further 3D classification. Two rounds of 3D classification were performed to identify the best-resolved subset of particles. This subset was subsequently subjected to 3D auto-refinement by projection matching in RELION. For 3D processing of the ATG2A dataset, the final ATG2A-WIPI4 reconstruction was used as an initial model after 60Å low-pass filtering. This data set was initially subjected to three rounds of 3D classification, and the best-resolved subset of particles was then subjected to 3D auto refinement. Smoothed binary 3D masks were generated from the final refined volumes, extending the mask density by five pixels and applying

an eight-pixel falloff. These masks were used to continue the 3D refinements to convergence. The final 3D reconstructions of ATG2A and the ATG2A-WIPI4 complex (Figs.1F and 1G) had an estimated resolution of 29.4 Å and 30.3 Å (Fig. S1) respectively, as assessed using Gold Standard Fourier Shell Correlation with a cutoff of 0.143. 6,386 and 5,317 particles contributed to the final reconstructions of ATG2A and the ATG2A-WIPI4 complex, respectively. 3D maps were visualized and segmented using UCSF Chimera (11). The homology model of human WIPI4 was built from a crystal structure of *Kluyveromyces lactis* Hsv2p (Protein Data Bank code: 4EXV) using the software Modeller (12) and docked into the ATG2A-WIPI4 density using UCSF Chimera.

Focused 2D analysis of the liposome-bound ATG2A-WIPI4 complexes was performed using a similar methodology as described in earlier work (13), with the ISAC (14) 2D classification program. In this process, initial reference-free 2D classification of all the particles resulted in classes depicting the ATG2-WIPI4 complex either tethering two liposomes or attached to a single liposome. Particles belonging to these two types of classes were separated into two sub-stacks, each of which was subjected to reference-free 2D alignment using "sxali2d" program of the SPARX EM data processing package (15). In this initial classification, the liposome electron microscopy density dominated the alignments. Based on the 2D averages of these aligned particles, binary masks were generated to eliminate density corresponding to the liposomes, enabling the 2D ISAC analyses to focus on the signal corresponding to the ATG2-WIPI4 complex. This resulted in class averages where the ATG2A-WIPI4 complexes were better resolved. The translational shifts and rotations determined in the masked analysis were then applied to the corresponding unmasked particles to generate unmasked 2D class averages containing well-resolved ATG2-WIPI4 complexes along with the associated liposomes (Fig. 3B (top row)). The ATG2-WIPI4 3D reconstructions were overlaid on these focused 2D class averages to annotate the different orientations of ATG2A (yellow density) -WIPI4 (green density) relative to the liposome (Fig. 3B (bottom row)).

Liposome flotation assay

Lipids (1,2-dioleoyl-*sn*-glycero-3-phosphocholine: DOPC and 1,2-dioleoyl-*sn*-glycero-3-phospho-L-serine: DOPS from Avanti Polar Lipids) and a dye, 1,1'-Dioctadecyl-3,3,3',3'-tetramethylindodicarbocyanine perchlorate (DiD) (Marker Gene Technologies), in chloroform were mixed at a molar ratio of DOPC/DOPS/DiD=99/0/1 or 74:25:1, or POPC/POPS/DiD=74/25/1, and dried under nitrogen gas. DiD was included to enable visualization of the liposomes. The obtained lipid films were further dried under vacuum for 15-60 minutes, followed by hydration with a buffer containing 20 mM Tris pH 7.5, and 150 mM NaCl. After hydration, the lipids were freeze-thawed seven times using liquid nitrogen and a 42˚C water bath. For SUVs, the lipids were sonicated for ~90 seconds using a probe-type sonicator until the solution becomes translucent. For LUVs, the lipids were extruded through a polycarbonate filter with a pore size of 30, 100 or 400 nm using an Avanti extruder. The flotation was carried out as reported previously (16). In brief, a 300 µL mixture solution of 50 nM ATG2A, 300 µM liposomes and 40% (w/v) Nycodenz (Accurate Chemical) in 20 mM Tris pH 7.5, 150 mM NaCl, and 0.5 mM TCEP was placed at the bottom of a centrifuge tube and a solution 250 µL of 30% Nycodenz in the same buffer was placed above the bottom solution. Finally, 50 µL of the same buffer without Nycodenz was placed on the top. The tubes were centrifuged in an SW55Ti rotor (Beckman Coulter) at 279,982 × *g* (max) for 4 hours at 20˚C. After the centrifugation, the liposomes were visible in the top layer. The top fractions (75 µL) containing all the liposomes were collected, and the contents were examined by SDS-PAGE. The gel was stained with Coomassie Brilliant Blue G-250 and scanned on LI-COR Odyssey infrared imaging system. The bands were quantified using Image Studio 2.0 software.

CXL-MS analysis

The CXL-MS analysis was carried out as described previously (17, 18). The ATG2A-WIPI4 complex was prepared at a concentration of 0.5 mg/ml in buffer containing 10 mM HEPES pH 7.5, 500 mM NaCl, 0.5 mM TCEP,

0.026 %(v/v) n-Dodecyl β-D-maltoside (DDM) and 20%(v/v) glycerol. For lysine-specific cross-linking, the pH was adjusted to 8.0 using 1 M HEPES pH 8.5. An equimolar mixture of DSS-d_0 and DSS-d_{12} (Creative Molecules Inc.) was added to the protein at a concentration of 0.25 mM and incubated at 37˚C for 30 min. For cross-linking of carboxyl groups and zero-length cross-linking, PDH-d_0/d_{10} and DMTMM (both from Sigma-Aldrich) were added to final concentrations of 8.3 and 12 mg/mL, respectively, and the samples were also incubated at 37 °C for 30 min. The cross-linking reactions were stopped by diluting the samples four-fold with DDM-free buffer and removing the excess of cross-linking reagents with the help of Zeba gel filtration spin desalting columns (7K MWCO, Thermo Scientific). This step also helped to remove DDM, which could interfere with further processing steps and MS analysis. The filtrate was dried in a vacuum centrifuge. Samples were reduced, alkylated, and digestion with endoproteinase Lys-C and trypsin according to standard procedures, and purified digests were separated by peptide-level size-exclusion chromatography (Supexdex Peptide 3.2/30, GE). SEC fractions were analyzed by LC-MS/MS on an Easy nLC-1000 HPLC system and an Orbitrap Elite mass spectrometer (both from ThermoFisher Scientific). Data analysis was performed using xQuest (19) against a database containing the sequences of ATG2A, WIPI4 and contaminant proteins (tubulins, heat shock proteins, and keratins).

DLS

DLS experiments were carried out with DynaPro Plate Reader II (Wyatt Technology). Solution mixtures containing 200 nM ATG2A and 60 μM (lipid) liposomes (75% DOPC/25% DOPS, or 75% DOPC/15% DOPS/10% 1,2-dioleoyl-*sn*-glycero-3-phospho-(1'-myo-inositol-3'-phosphate) (PI3P)) in buffer 20 mM HEPES pH 7.5, 150 mM NaCl, and 0.5 mM TCEP were incubated for an hour at 25˚C, followed by the DLS measurements with a laser power of 10%. In this condition, the protein alone did not produce measurable scattering, confirming that the DLS signals were from liposomes. Proteinase K (Sigma) was added to the clustered sonicated liposomes at a final concentration of 20 μg/ml, and the DLS was measured after 1 and 2 hours. All data were analyzed in the program DYNAMICS included in the instrument.

Fluorescence liposome tethering assay

Fluorescence liposome tethering assays were performed similarly as described previously (20). For the experiments monitoring the tethering by ATG2A alone as shown in Figs. 4 and 7, two kinds of liposomes were prepared. One comprised 73.3% DOPC, 25% DOPS, 0.2% 1,2-distearoyl-*sn*-glycero-3-phosphoethanolamine-N-[biotinyl(polyethylene glycol)-2000] (DSPE-PEG(2000)-Biotin) and 1.5% 1,2-dioleoyl-*sn*-glycero-3-phosphoethanolamine-N-(lissamine rhodamine B sulfonyl) (Rhod-PE), and the other 73% DOPC, 25% DOPS and 2% DiD. SUVs and LUVs were prepared from each lipid mixture by sonication or extrusion. The former and the latter liposomes with the same size were mixed at a concentration of 60 μM (lipid) each in the presence or absence of 100 nM ATG2A. The mixture was incubated at room temperature for 5 min. Streptavidin MagneSphere resin (PROMEGA) was then added to the mixture. After 5 min incubation, the resin was washed five times and resuspended in methanol. DiD fluorescence was normalized against rhodamine fluorescence to correct the difference of the total liposomes absorbed on the beads. For the experiments with PI3P and WIPI4 as shown in Figs. 5 and 7, LUVs with a lipid composition of 73.3% DOPC, 15% DOPS, 10% PI3P, 0.2% DSPE-PEG(2000)-Biotin and 1.5% Rhod-PE were mixed with those of 73% DOPC, 25% DOPS and 2% DiD.

CD spectroscopy

SUVs comprised of 75% DOPC and 25% DOPS were prepared by sonication and mixed with MBP-CLR at a molar ratio of protein:lipid=1:50. MBP was cleaved off by TEV protease, and the protein-SUV complex was purified by Nycodenz flotation as described above. The top fraction was dialyzed against the CD buffer consisting of 10 mM

potassium phosphate pH 7.4, 150 mM potassium fluoride. After the dialysis, the sample was put into a cuvette with a path length of 1 mm. The final sample contained 6.7 μM CLR. The spectrum was acquired on an Aviv spectrophotometer at 25˚C. A sample containing only SUVs (335 μM lipid) was measured, and the resulting spectrum was used for background subtraction. The secondary structure contents were estimated by the program K2D3 (21).

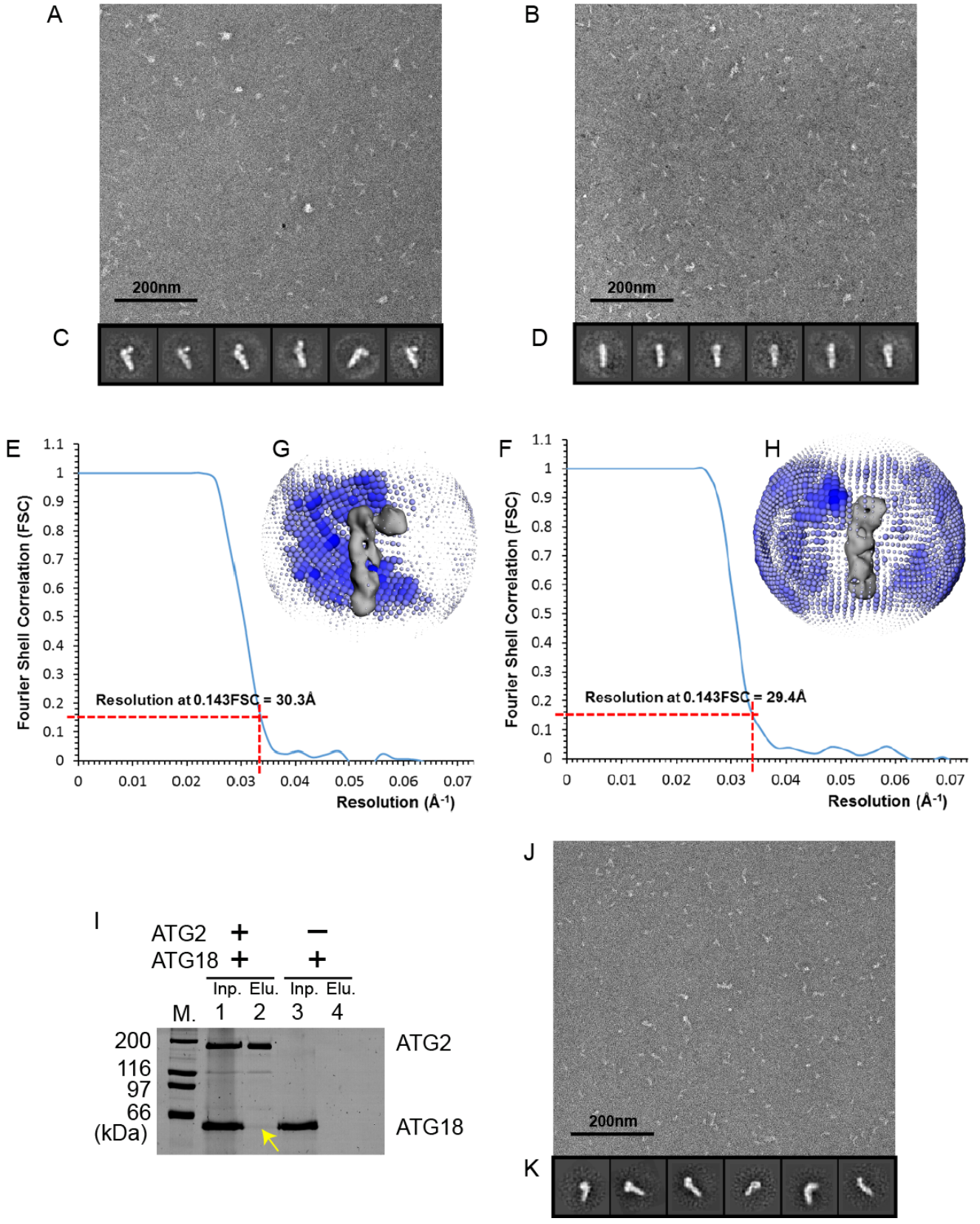
A
200nm
C
B
200nm
D
E
G
Fourier Shell Correlation (FSC)
Resolution at 0.143FSC = 30.3Å
Resolution (Å-1)
F
H
Fourier Shell Correlation (FSC)
Resolution at 0.143FSC = 29.4Å
Resolution (Å-1)
I
ATG2 + −
ATG18 + +
Inp. Elu. Inp. Elu.
M. 1 2 3 4
200
116
97
66
(kDa)
ATG2
ATG18
J
200nm
K

Fig. S1. Negative-stain EM analyses of the human ATG2A-WIPI4 complex, free human ATG2A, and *Sc*ATG2-ATG18 complex. (A, B) Representative electron micrographs of the ATG2A-WIPI4 complex (A) and free ATG2A (B) stained with 2% uranyl formate. (C, D) 2D class averages of the ATG2A-WIPI4 complex (C) and free ATG2A (D). (E, F) Fourier Shell Correlation (FSC) curves of the 3D reconstructions of the ATG2A-WIPI4 complex (E) and free ATG2A. (G, H) Euler angle distributions of the particles used for the final 3D reconstructions of the ATG2A-WIPI4 complex (G) and free ATG2A (H). (I) An affinity capture experiment with *Sc*ATG2 immobilized on beads (Strep-Tactin) and *Sc*ATG18 in solution. The experiment was performed as described in Methods for the same experiment with human proteins. Although the band of *Sc*ATG18 in the elution from the beads loaded with *Sc*ATG2 (lane2; indicated by an arrow) is faint, such band is completely absent in the control without *Sc*ATG2 (lane 4), allowing us to conclude that the *Sc*ATG18 band in the lane 2 is the proteins bound to *Sc*ATG2. (J) A representative electron micrograph of the negatively stained elution sample of (I). (K) 2D class averages of the *Sc*ATG2-ATG18 complex.

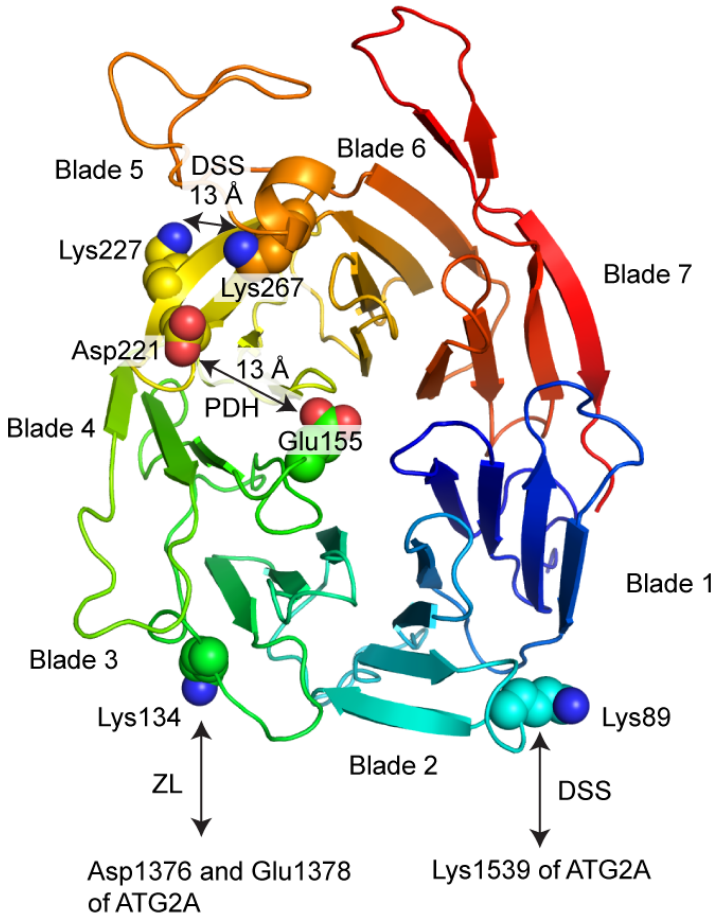

Fig. S2. Cross-linked positions of WIPI4. The residues cross-linked within WIPI4 or with ATG2A are shown with their side chains on the WIPI4 homology model. The two residues cross-linked by DSS (Lys227 and Lys267) or PDH (Glu155 and Asp221) are both ~13 Å apart, which is within reach of each cross-linker.

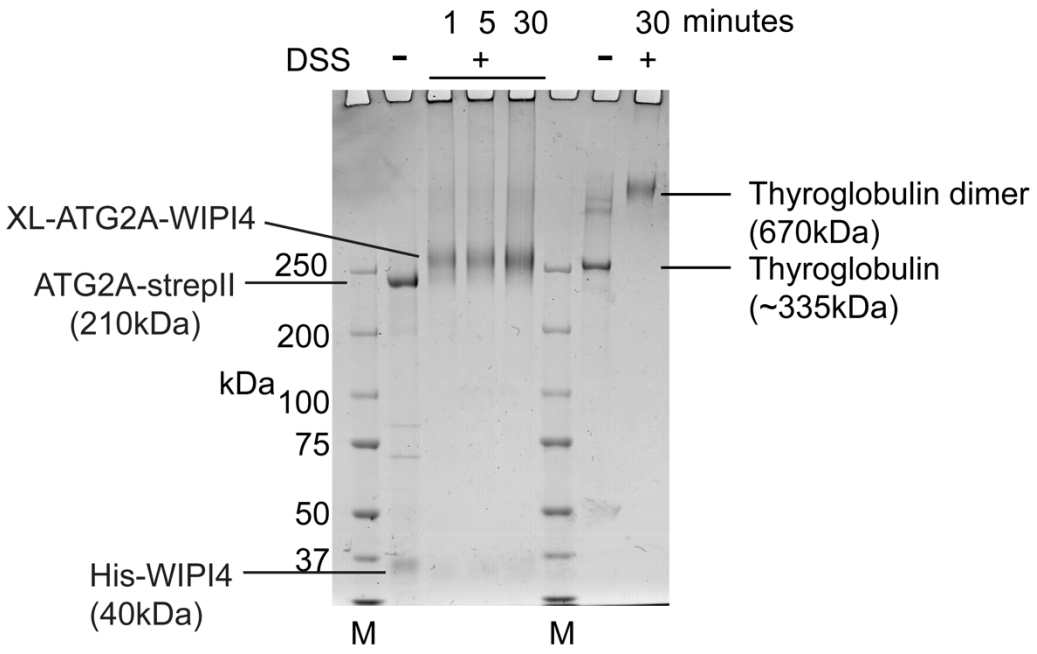

Fig. S3. SDS-PAGE analysis of DSS-cross-linking between ATG2A and WIPI4. A positive control reaction with ~350kDa thyroglobulin is shown in right.

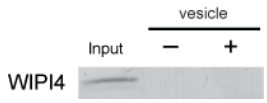

Fig. S4. WIPI4 does not bind to the liposomes used for the negative stain EM study for the ATG2A-WIPI4-SUV complex shown in Fig. 3. Flotation assay with WIPI4 was performed with 75%DOPC/25%DOPS liposome generated by dialysis as described in the main text. The result shows no binding of WIPI4 to these liposomes.

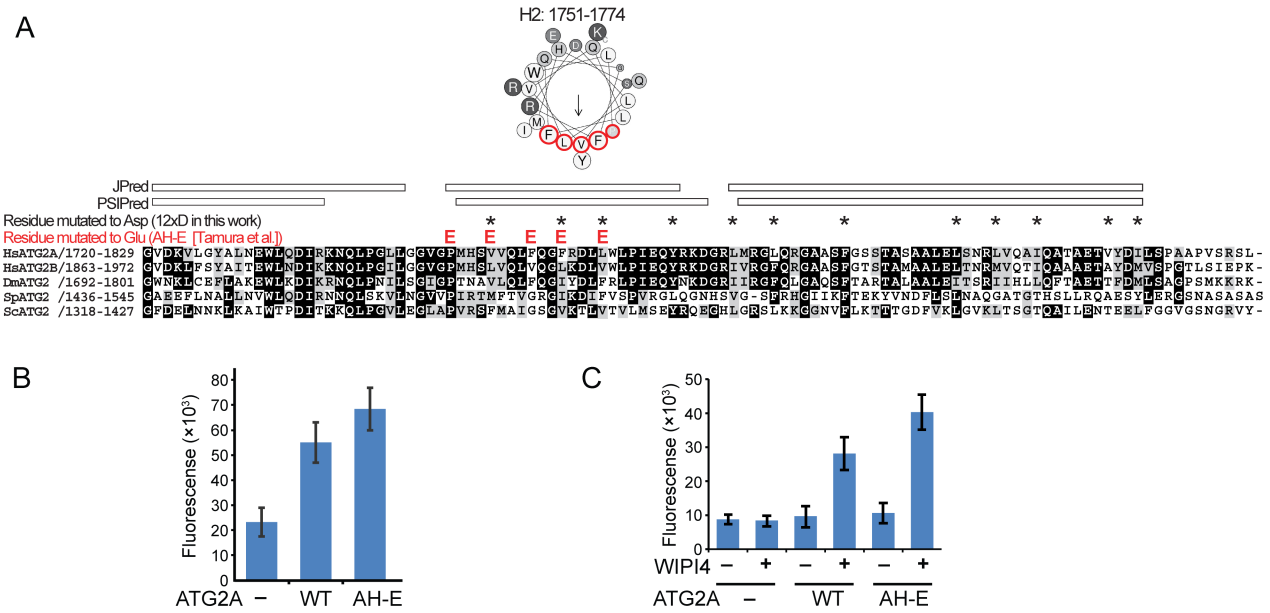

Fig. S5. The AH-E mutation in the full-length ATG2A protein do not affect membrane tethering. (A) The positions of the five residues in H2 that were mutated to glutamic acid by Tamura et al. (22) are indicated by red circles in the cartwheel drawing of H2 and also indicated above the sequence alignment. Three of the five residues are the same in our ATG2A^{12xD} construct. (B, C) Fluorescence homotypic (B) and heterotypic (C) membrane tethering assays with wild-type and AH-E mutant of ATG2A. The experiments were performed in the same manner as in Fig. 4F and 5F.

Table S1: List of cross-linked peptide fragments identified by CXL-MS

Linker	Id	Protein 1	Protein 2	AbsPos 1	AbsPos 2	AA length (distance)	Id-Score
DSS (Lys-Lys)	EGVAKAYDTVR-SLQDKR-a5-b5	ATG2A	ATG2A	1853	1832	21	33.87
	GTVHIFALKDTR-EKLVELR-a9-b2	WIPI4	WIPI4	267	227	40 (~13Å)	33
	EGVAKAYDTVR-VSKALDPK-a5-b3	ATG2A	ATG2A	1853	720	1133	29.83
	GHEQKGLTGAVGGVIR-SLQDKR-a5-b5	ATG2A	ATG2A	1880	1832	48	29.12
	GHEQKGLTGAVGGVIR-EGVAKAYDTVR-a5-b5	ATG2A	ATG2A	1880	1853	27	29.07
	VSKALDPK-SLQDKR-a3-b5	ATG2A	ATG2A	720	1832	1112	28.63
	LASSQINKFLYLHTSER-SLQDKR-a8-b5	ATG2A	ATG2A	1539	1832	293	28.09
	NQIVPDAHKDHALK-EGVAKAYDTVR-a9-b5	ATG2A	ATG2A	1925	1853	72	28.02
	NQIVPDAHKDHALK-SLQDKR-a9-b5	ATG2A	ATG2A	1925	1832	93	27.64
	GHEQKGLTGAVGGVIR-NQIVPDAHKDHALK-a5-b9	ATG2A	ATG2A	1880	1925	45	26.65
	LASSQINKFLYLHTSER-EGKDSK-a8-b3	ATG2A	WIPI4	1539	89	–	26.32
	ALDPKSTGR-SLQDKR-a5-b5	ATG2A	ATG2A	725	1832	1107	25.6
	GHEQKGLTGAVGGVIR-VSKALDPK-a5-b3	ATG2A	ATG2A	1880	720	1160	20.96
PDH (Asp/Glu-Asp/Glu)	LRFPIADLRPER-AEQLR-a11-b2	ATG2A	ATG2A	655	667	12	30.11
	FPIADLRPER-AEQLR-a9-b2	ATG2A	ATG2A	655	667	12	27.31
	GLCDLCPSLEK-LFDTQSK-a10-b3	WIPI4	WIPI4	155	221	66 (~13Å)	27.15
ZL (Lys-Asp/Glu)	DGEPVVTQLHPGPIVVR-KLFEFDTR-a3-b1	ATG2A	WIPI4	1378	134	–	30.45
	IKVTFLDTVVR-VEHSPGDGER-a2-b2	ATG2A	ATG2A	168	179	11	25.43
	EPEPSPFSSK-ALDPKSTGR-a3-b5	ATG2A	ATG2A	773	725	48	21.06
	DGEPVVTQLHPGPIVVR-KLFEFDTR-a1-b1	ATG2A	WIPI4	1376	134	–	20.94

Id; Assigned peptides and cross-linking sites within the *peptide* sequences. The longer peptide is designated as (a)lpha, the shorter as (b)eta. *Protein1*; The protein containing peptide designated as alpha. *Protein2*; The protein containing peptide designated as beta. *AbsPos1*; Position in the protein sequence of protein 1. *AbsPos2*; Position in the protein sequence of protein 2. *AA length (distance)*; Number of amino acid residues between AbsPos1 and AbsPos2. Distances between the two residues in the WIPI4 homology model are noted in parentheses. *Id-score*; Identification score as assigned by xQuest.

Movie S1. WIPI4 (round lobe) is flexibly attached to ATG2 (rod-like density), as shown by aligning 2D averages of the complex to the density corresponding to ATG2.

References

1. Bieniossek C, Imasaki T, Takagi Y, & Berger I (2012) MultiBac: expanding the research toolbox for multiprotein complexes. *Trends Biochem Sci* 37(2):49-57.
2. Suloway C*, et al.* (2005) Automated molecular microscopy: the new Leginon system. *J Struct Biol* 151(1):41-60.
3. Lander GC*, et al.* (2009) Appion: an integrated, database-driven pipeline to facilitate EM image processing. *J Struct Biol* 166(1):95-102.
4. Mindell JA & Grigorieff N (2003) Accurate determination of local defocus and specimen tilt in electron microscopy. *J Struct Biol* 142(3):334-347.
5. Voss NR, Yoshioka CK, Radermacher M, Potter CS, & Carragher B (2009) DoG Picker and TiltPicker: software tools to facilitate particle selection in single particle electron microscopy. *J Struct Biol* 166(2):205-213.
6. Ludtke SJ, Baldwin PR, & Chiu W (1999) EMAN: semiautomated software for high-resolution single-particle reconstructions. *J Struct Biol* 128(1):82-97.
7. Ogura T, Iwasaki K, & Sato C (2003) Topology representing network enables highly accurate classification of protein images taken by cryo electron-microscope without masking. *J Struct Biol* 143(3):185-200.
8. Yoshioka C, Lyumkis D, Carragher B, & Potter CS (2013) Maskiton: Interactive, web-based classification of single-particle electron microscopy images. *J Struct Biol* 182(2):155-163.
9. Scheres SH (2012) RELION: implementation of a Bayesian approach to cryo-EM structure determination. *J Struct Biol* 180(3):519-530.
10. Shaikh TR*, et al.* (2008) SPIDER image processing for single-particle reconstruction of biological macromolecules from electron micrographs. *Nat Protoc* 3(12):1941-1974.
11. Goddard TD, Huang CC, & Ferrin TE (2007) Visualizing density maps with UCSF Chimera. *J Struct Biol* 157(1):281-287.
12. Webb B & Sali A (2014) Comparative Protein Structure Modeling Using MODELLER. *Curr Protoc Bioinformatics* 47:5 6 1-32.
13. Chowdhury S, Ketcham SA, Schroer TA, & Lander GC (2015) Structural organization of the dynein-dynactin complex bound to microtubules. *Nat Struct Mol Biol* 22(4):345-347.
14. Yang Z, Fang J, Chittuluru J, Asturias FJ, & Penczek PA (2012) Iterative stable alignment and clustering of 2D transmission electron microscope images. *Structure* 20(2):237-247.
15. Hohn M*, et al.* (2007) SPARX, a new environment for Cryo-EM image processing. *J Struct Biol* 157(1):47-55.
16. Nath S*, et al.* (2014) Lipidation of the LC3/GABARAP family of autophagy proteins relies on a membrane-curvature-sensing domain in Atg3. *Nat Cell Biol* 16(5):415-424.
17. Leitner A, Walzthoeni T, & Aebersold R (2014) Lysine-specific chemical cross-linking of protein complexes and identification of cross-linking sites using LC-MS/MS and the xQuest/xProphet software pipeline. *Nat Protoc* 9(1):120-137.
18. Leitner A*, et al.* (2014) Chemical cross-linking/mass spectrometry targeting acidic residues in proteins and protein complexes. *Proc Natl Acad Sci U S A* 111(26):9455-9460.
19. Walzthoeni T*, et al.* (2012) False discovery rate estimation for cross-linked peptides identified by mass spectrometry. *Nat Methods* 9(9):901-903.
20. Ragusa MJ, Stanley RE, & Hurley JH (2012) Architecture of the Atg17 complex as a scaffold for autophagosome biogenesis. *Cell* 151(7):1501-1512.

21. Louis-Jeune C, Andrade-Navarro MA, & Perez-Iratxeta C (2012) Prediction of protein secondary structure from circular dichroism using theoretically derived spectra. *Proteins* 80(2):374-381.
22. Tamura N*, et al.* (2017) Differential requirement for ATG2A domains for localization to autophagic membranes and lipid droplets. *FEBS Lett* 591(23):3819-3830.